RESEARCH ARTICLE SUMMARY

DNA NANOTECHNOLOGY

Reconfiguration of DNA molecular arrays driven by information relay

Jie Song,*† Zhe Li,* Pengfei Wang,* Travis Meyer, Chengde Mao,† Yonggang Ke†

INTRODUCTION: Information relay at the molecular level is an essential phenomenon in numerous chemical and biological processes. A key challenge in synthetic molecular self-assembly is to construct artificial structures that imitate these complex dynamic behaviors in controllable systems. One promising route is DNA self-assembly, a potent approach for the design and construction of arbitrary-shaped artificial nanostructures with increasing complexity and precision. Nonetheless, despite recent progress in the construction of reconfigurable DNA nanostructures that undergo tailored post-assembly transformations in response to different physical or chemical cues, the dynamic behaviors of massive, complex DNA structures remain limited. The existing systems typically exhibit relatively simple dynamic behaviors that involve a single step or a few steps of transformation. Moreover, many of these structures contain mainly static segments joined by a few small reconfigurable domains.

RATIONALE: Here, we demonstrated prescribed, long-range information relay in artificial molecular arrays assembled from modular DNA antijunction units. The small dynamic antijunction unit contains four DNA double-helix domains of equal length and four dynamic nicking points, and can switch between two stable conformations, through an intermediate open conformation. In an array, the driving force of information relay is base stacking: The conformational switch of one antijunction unit will cause the interface between the transformed unit and its neighboring units to become a high-energy conformation with weakened base stacking, leading to transformations in the neighboring units. The array transformation is equivalent to a molecular "domino array": Once initiated at a few selected units, the transformation then propagates, without the addition of extra "trigger strands," to neighboring units and eventually the entire array. The specific information pathways by which this transformation occurs can be controlled by adding trigger strands to specific units, or by altering the design of individual units, the connections between units, and the geometry of the array.

RESULTS: The reconfigurable DNA relay arrays were constructed by using both origami and single-strand–brick approaches. In one-pot assembly, we observed that the arrays built from antijunction units exhibited a spectrum of shapes to accommodate different combinations of antijunction conformations. With the incorporation of set strands, we could lock the arrays into prescribed conformations. The more set strands were added, the greater the assembly shifted toward the corresponding array conformation. Other factors, including the size and aspect ratio of an array, the connecting pattern of an array, DNA sequences of an array, cation concentration, and temperature, have been shown to affect the result of one-pot assembly.

ON OUR WEBSITE

Read the full article at http://dx.doi.org/10.1126/science.aan3377

The transformation cascade was demonstrated with preassembled arrays. When starting from one conformation, addition of the trigger strand at selected locations of the array initiates structural transformation from the selected sites and propagates to the rest of the array in a stepwise manner without additional trigger strands at other locations. Releasing the old trigger strands and adding new ones can transform the array back to its initial conformation—a reversible process that can be repeated multiple rounds. In addition, we were able to control the propagation pathway to follow prescribed routes, as well as to stop and then resume propagation by mechanically decoupling the antijunctions or introducing "block strands." The kinetics of array transformation can be enhanced by elevated temperature or formamide. These assembly and transformations were studied mainly by atomic force microscopy and native agarose gel electrophoresis.

CONCLUSION: Our work demonstrates controlled, multistep, long-range transformation in DNA nanoarrays, assembled by interconnected modular dynamic units that can transfer their structural information to neighbors. The array's dynamic behavior can be regulated by external factors, the shapes and sizes of arrays, the initiation of transformation at selected units, and the engineered information propagation pathways. We expect that the DNA relay arrays will shed new light on how to construct nanostructures with increasing size and complex dynamic behaviors, and may enable a range of applications, such as the construction of molecular devices to detect and translate molecular interactions to conformational changes in DNA structures, to remotely trigger subsequent molecular events. ■

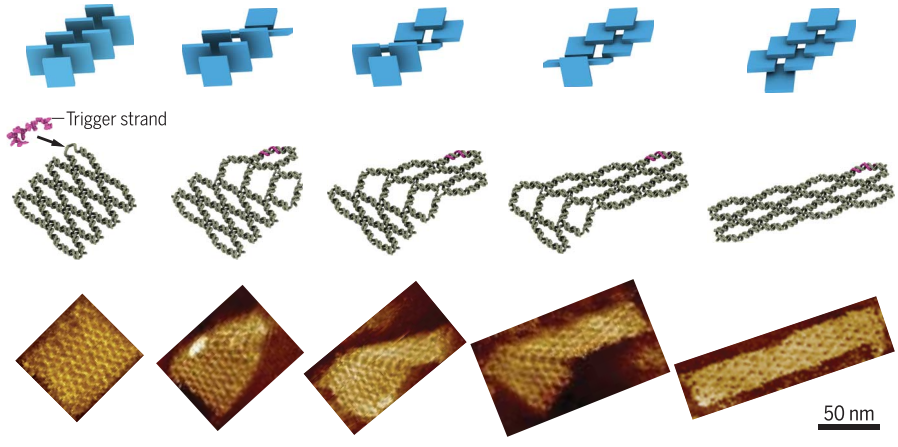

Information relay in DNA "domino" nanoarrays. In a manner similar to that of domino arrays (top), the molecular DNA nanoarray transforms in a step-by-step relay process, initiated by the hybridization of a trigger strand to a single unit (middle). Different stages of nanoarray transformation were confirmed by AFM (bottom). Scale bar, 50 nm.

The list of author affiliations is available in the full article online.
*These authors contributed equally to this work.
†Corresponding author. Email: yonggang.ke@emory.edu (Y.K.); sjie@sjtu.edu.cn (J.S.); mao@purdue.edu (C.M.)
Cite this article as J. Song *et al.*, *Science* **357**, eaan3377 (2017). DOI: 10.1126/science.aan3377

RESEARCH ARTICLE

DNA NANOTECHNOLOGY

Reconfiguration of DNA molecular arrays driven by information relay

Jie Song,[1,2]*† Zhe Li,[3]* Pengfei Wang,[1]* Travis Meyer,[1]
Chengde Mao,[3]† Yonggang Ke[1,4]†

Information relay at the molecular level is an essential phenomenon in numerous chemical and biological processes, such as intricate signaling cascades. One key challenge in synthetic molecular self-assembly is to construct artificial structures that imitate these complex behaviors in controllable systems. We demonstrated prescribed, long-range information relay in an artificial molecular array assembled from modular DNA structural units. The dynamic DNA molecular array exhibits transformations with programmable initiation, propagation, and regulation. The transformation of the array can be initiated at selected units and then propagated, without addition of extra triggers, to neighboring units and eventually the entire array. The specific information pathways by which this transformation occurs can be controlled by altering the design of individual units and the arrays.

Molecular self-assembly has played a crucial role in bottom-up fabrication of materials across many length scales. Structural DNA nanotechnology (*1*) has proved to be a potent approach for the design and construction of arbitrarily shaped artificial nanostructures, including static and dynamic structures, largely because of the programmability of this versatile biomolecule. The field has produced diverse, custom-shaped DNA nanostructures, including one-dimensional (1D) ribbons (*2*–*4*) and tubes (*2*, *4*–*10*), 2D lattices (*5*, *10*–*16*), and finite 2D and 3D objects with prescribed shapes (*14*, *17*–*30*).

The basic principle of DNA nanostructure design is to engineer structural information into the DNA sequences by programming complementarity between component DNA strands (*1*). The present approaches for constructing DNA nanostructures largely fall into two major categories: DNA origami and DNA tiles. DNA origami is a "folding" method, in which a long "scaffold" strand (often M13 viral genomic DNA) is folded into a prescribed shape via interactions with hundreds of short, synthetic "staple" strands (*20*). The DNA tile method assembles DNA structures by connecting small structural units, typically consisting of a small number of strands (*11*). The DNA origami approach has produced fully addressable structures up to several thousands of base pairs (bp) (*7*). Similar-sized, fully addressable structures have also been fabricated with special types of DNA tiles, such as single-stranded tiles (*4*, *26*) or DNA bricks (*27*).

Besides engineering intricate static structures, DNA has also been used to fabricate dynamic structures with tailored postassembly transformations—another important advantage of self-assembly from information-rich biomolecules. Many dynamic DNA devices have been demonstrated, including tweezers (*31*–*34*), walkers (*35*–*40*), reconfigurable arrays assembled from simple DNA tile units (*41*), and other complex devices (*14*, *42*, *43*). These devices can sense a range of physical or chemical cues. Nonetheless, the dynamic behaviors of massive, complex DNA structures are still limited. The existing systems typically exhibit relatively simple dynamic behaviors that involve a single step or a few steps of transformation. Moreover, despite their massive size, many dynamic DNA origami structures were designed to contain mainly static segments joined by a few small dynamic regions (*14*, *42*, *43*).

Here we demonstrate programmable molecular information cascades formed by DNA arrays, which simulate some of the key aspects of complex biological signaling cascades, such as initiation, propagation, and regulation observed in signaling cascades initiated by T cell receptor binding. (*44*) Our large, scalable DNA array is analogous to a molecular "domino array": the step-by-step transformation propagates through the interconnected DNA units via specifically prescribed pathways (fig. S1). We show that the reversible transformation of a DNA array can be initiated at designated locations, and follows pathways precisely controlled by programming the shape of the array or by adding molecular switches that block and then resume the information relay between units.

Design of DNA relay arrays

We used small dynamic DNA units called "antijunctions" (*45*) to build large, scalable, reconfigurable DNA structures. An antijunction contains four DNA duplex domains of equal length and four dynamic nicking points (Fig. 1, A and B; note that the strand in gray contains a static nick, which does not change during reconfiguration). This small construct can switch between two stable conformations—"red" and "green," driven by base-stacking, through an unstable open (including partially open) conformation—"orange." Each duplex is $0.5 \times n$ turns (n = 1, 2, 3, 4...) in length (fig. S2A). An antijunction is classified by the distance between two opposite dynamic nicking points (i.e., a 42-bp antijunction).

In a connected network, the conformational information of an antijunction can pass to its closest neighbors, introducing subsequent conformational change of the neighboring antijunctions (Fig. 1C). The transformation of an individual antijunction unit (e.g., from red to green) can be induced by adding a trigger DNA strand that forms a continuous duplex on one edge of the unit (fig. S3A). The key design feature of trigger strands is that each trigger strand removes a mobile nick point from an antijunction unit. After the conformational switch from red to green of the triggered unit, the interface between the two neighboring units becomes a high-energy open conformation, leading to a transformation in the neighboring unit to the same conformation (green) as the already transformed unit. This process is driven by the reduction of free energy, caused by the formation of an additional base-stacking interaction at the connection point (see fig. S3B for more details).

We built 2D molecular DNA relay array via self-assembly of the antijunctions (Fig. 1D). A relay array can transform from one array conformation (e.g., all antijunctions are in the red conformation) to another array conformation (e.g., all antijunctions are in the green conformation). The array transformation follows specific pathways, depending on the array's geometry and binding locations of trigger strands (fig. S4). For instance, if the trigger strands were added to the units (Fig. 1, D and E) at a corner, the relay would undergo a step-by-step conversion from a red array conformation to a green array conformation via a diagonal pathway.

DNA relay arrays can be constructed with both noncanonical DNA bricks (single-stranded modular DNA units) and DNA origami (further discussion is in figs. S5 to S8). Owing to the constraint of the continuous scaffold, a DNA-origami antijunction must be an odd-number-turn antijunction (e.g., 32-bp antijunction; figs. S5 and S7). In comparison, a DNA-brick antijunction can be either an odd-number-turn antijunction (e.g., 32-bp antijunction; figs. S5 and S7) or an even-number-turn antijunction (e.g., 42-bp antijunction; figs. S6 and S8). One of the array conformations of the DNA-brick arrays is arbitrarily assigned as

[1]Coulter Department of Biomedical Engineering, Emory University and Georgia Institute of Technology, Atlanta, GA 30322, USA. [2]Department of Instrument Science and Engineering, School of Electronic Information and Electrical Engineering, Shanghai Jiaotong University, Shanghai 200240, China. [3]Department of Chemistry, Purdue University, West Lafayette, IN 47907, USA. [4]Department of Chemistry, Emory University, Atlanta, GA 30322, USA.
*These authors contributed equally to this work. †Corresponding author. Email: yonggang.ke@emory.edu (Y.K.); sjie@sjtu.edu.cn (J.S.); mao@purdue.edu (C.M.)

the red array conformation, and the other is assigned as the green array conformation (fig. S5, B and D). For DNA-origami relay arrays, the conformation where the scaffold does not cross between DNA helices within the array is assigned as the red array conformation, and the other conformation is assigned as the green conformation (fig. S5, C and E).

One-pot assembly of DNA-brick relay arrays

The transformation pathway of a DNA relay array is expected to be dictated by the stable conformations corresponding to local energy minima. To investigate these local energy-minimum states, we first studied the self-assembly of rectangular 42-bp DNA-brick relay arrays via one-pot isothermal assembly. The results revealed that the most dominant conformations were the red array conformation and the green array conformation. In addition to the two dominant conformations, which should correspond to the two lowest-energy states, we observed many mixed-conformation arrays that consist of both regions of red antijunctions and regions of green antijunctions. We observed that the red antijunction regions and the green antijunction regions were always bridged by a diagonal seam(s) that contains open orange antijunctions. These orange antijunctions are unstable by themselves, but can exist in an array structure when they are flanked by red antijunctions and green antijunctions (Fig. 2A). These arrays with mixed antijunction conformations are called "mixed array" conformations, which correspond to local energy minima in the assembly (Fig. 2B). Further discussion of these stable mixed array conformations is in fig. S9.

Native agarose gel electrophoresis of a rectangular 20 unit by 4 unit (20 × 4) 42-bp DNA-brick relay array revealed two product bands that correspond to the red array conformation and the green array conformation, respectively (Fig. 2C). The green array conformation showed greater mobility than the red array conformation, likely due to its elongated geometry. The mixed array conformations contain many different shapes that do not migrate as a single band, but were observed in atomic force microscopy (AFM) images of unpurified samples (Fig. 2D).

An 11 × 4 42-bp DNA-brick relay array was used to test optimal assembly conditions (fig. S10). The best yield was observed when the array was assembled at 51.3°C isothermally, in a Tris-EDTA (TE) buffer containing 10 mM $MgCl_2$. Addition of single-stranded poly-T extensions around the boundary of the array further improved the yield (fig. S11), presumably due to the poly-T's function of mitigating unwanted aggregation (*20*).

Regulation of assembly of DNA-brick relay arrays

To understand how size and aspect ratio affect the assembly of DNA relay array, we tested the one-pot assembly of a group of rectangular 42-bp DNA-brick relay arrays. The largest structure is a 20 × 8 DNA-brick array consisting of randomly generated ~14,000 bp (Fig. 2E). In total, 16 DNA-brick relay arrays with different sizes and aspect ratios were generated by using the 20 × 8 relay array as a molecular canvas (Fig. 2F and fig. S12). Native agarose gel electrophoresis and AFM images

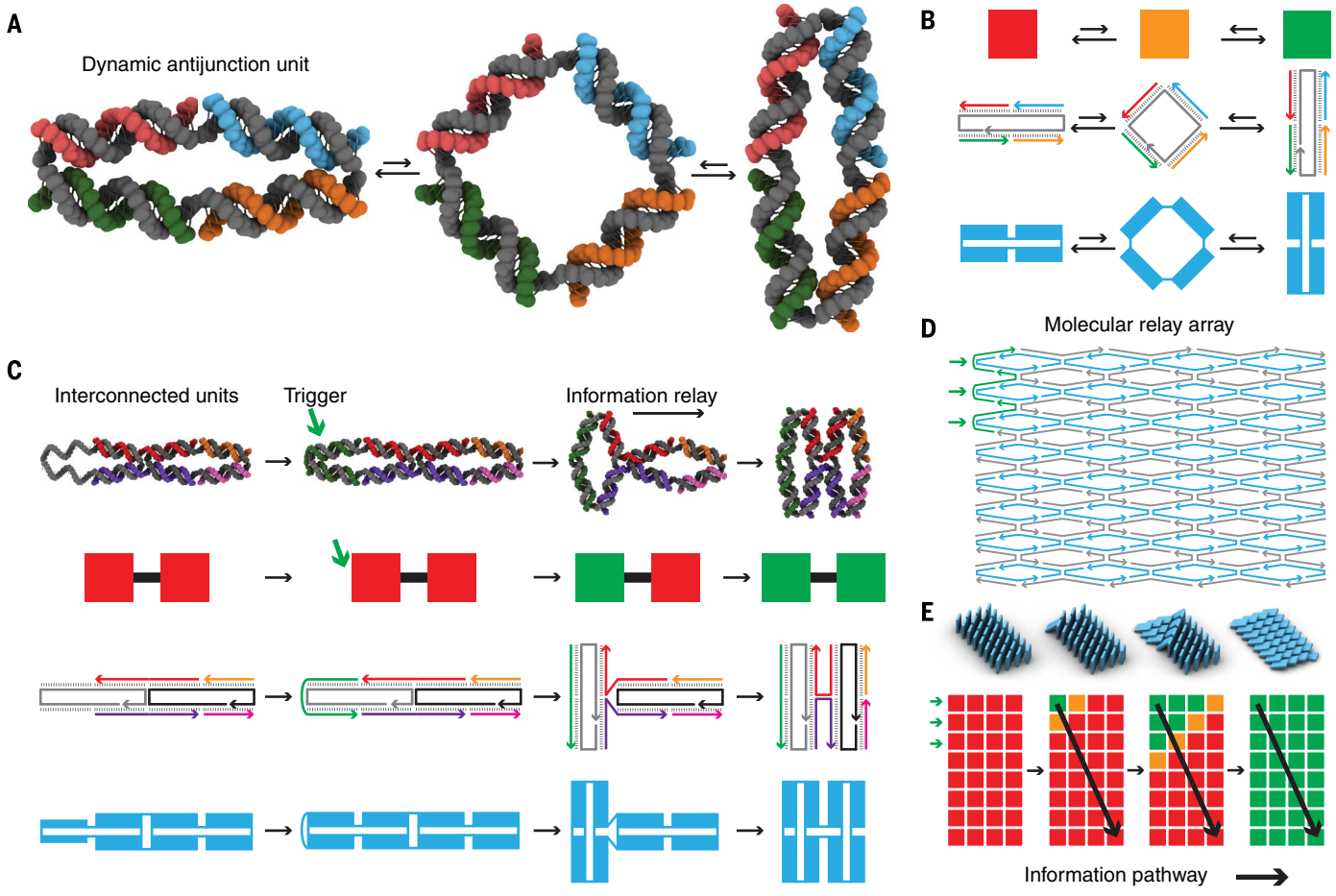

Fig. 1. Molecular relay arrays assembled by DNA. (**A**) A dynamic DNA antijunction can switch between two stable conformations, through an unstable open conformation. (**B**) Different diagrams for a DNA antijunction: stable conformations "red" and "green," and unstable conformation "orange." (**C**) Transformation of an antijunction unit can be induced by addition of a trigger strand. The information is passed from the converted unit to its closest neighbors, causing them to undergo subsequent transformation. (**D**) Strand diagram of an interconnected 2D DNA relay array with 4 units by 8 units. Three trigger strands (green) are added to three units in the upper-left corner of the array to initiate the transformation (**E**) The information of transformation propagates along prescribed pathways, causing the units to convert sequentially in this molecular array.

(figs. S13 and S14) were used to analyze the percentages of the red array conformation, the green array conformation, and the mixed array conformation of the 16 structures (Fig. 2F, fig. S15, and table S1). All relay arrays produced a large amount of both the red arrays and the green arrays, except for the $n \times 2$ arrays, whose assembly appeared to favor the larger–aspect ratio green array conformation, suggesting that aspect ratios play a more important role for this group of structures. Our analysis, using a simple proximity model (fig. S16) that considered only the energy between the closest neighboring helices, showed that the array's aspect ratios had a larger effect on the $n \times 2$ arrays, consistent with the above observation.

We then studied how the one-pot assembly of arrays was affected by the presence of trigger strands, connection patterns between units, and the DNA sequences. In the first test, the addition of a few trigger strands in the one-pot assembly clearly altered the R/G ratios for the 11 × 4 42-bp DNA-brick relay array (Fig. 2G and table S2). As expected, the more trigger strands were added to the one-pot assembly, the further the assembly shifted toward the corresponding array conformation.

Changing the connectivity between antijunction units also affects the assembly of the 11 × 4 42-bp DNA-brick relay array (Fig. 2H and fig. S17). When antijunction units were removed from the 11 × 4 42-bp DNA-brick relay array, the assembly shifted to more green array conformations (Fig. 2H), probably because of the increasing narrow (1.5 units in width) areas, which favor a green array conformation.

In comparison to the results in Fig. 2G, assembly of the 11×4 42-bp DNA brick relay array with missing units in the presence of eight red trigger strands resulted in a more mixed array conformation, likely because the reduced connectivity also diminishes the effectiveness of trigger strands (Fig. 2I). This effect is particularly pronounced with the 11 × 4 42-bp DNA brick relay array with two holes—about half of the arrays formed a "mask"-shaped mixed array conformation (fig. S18). Statistics of the 11 × 4 42-bp DNA brick relay array with modified connectivity are shown in table S3, and additional studies on controlling the one-pot assembly of DNA-brick relay arrays are included in fig. S19.

Considering that the change of base stacking occurs only at each four-way junction, the DNA sequences at the junctions may play an important role in determining the assembly results. To verify this hypothesis, we tested two versions of the 11 × 4 42-bp DNA-brick relay arrays with modified sequences at the junctions (fig. S20). The two arrays (design I and II) have the same sequences, except for the eight DNA bases at

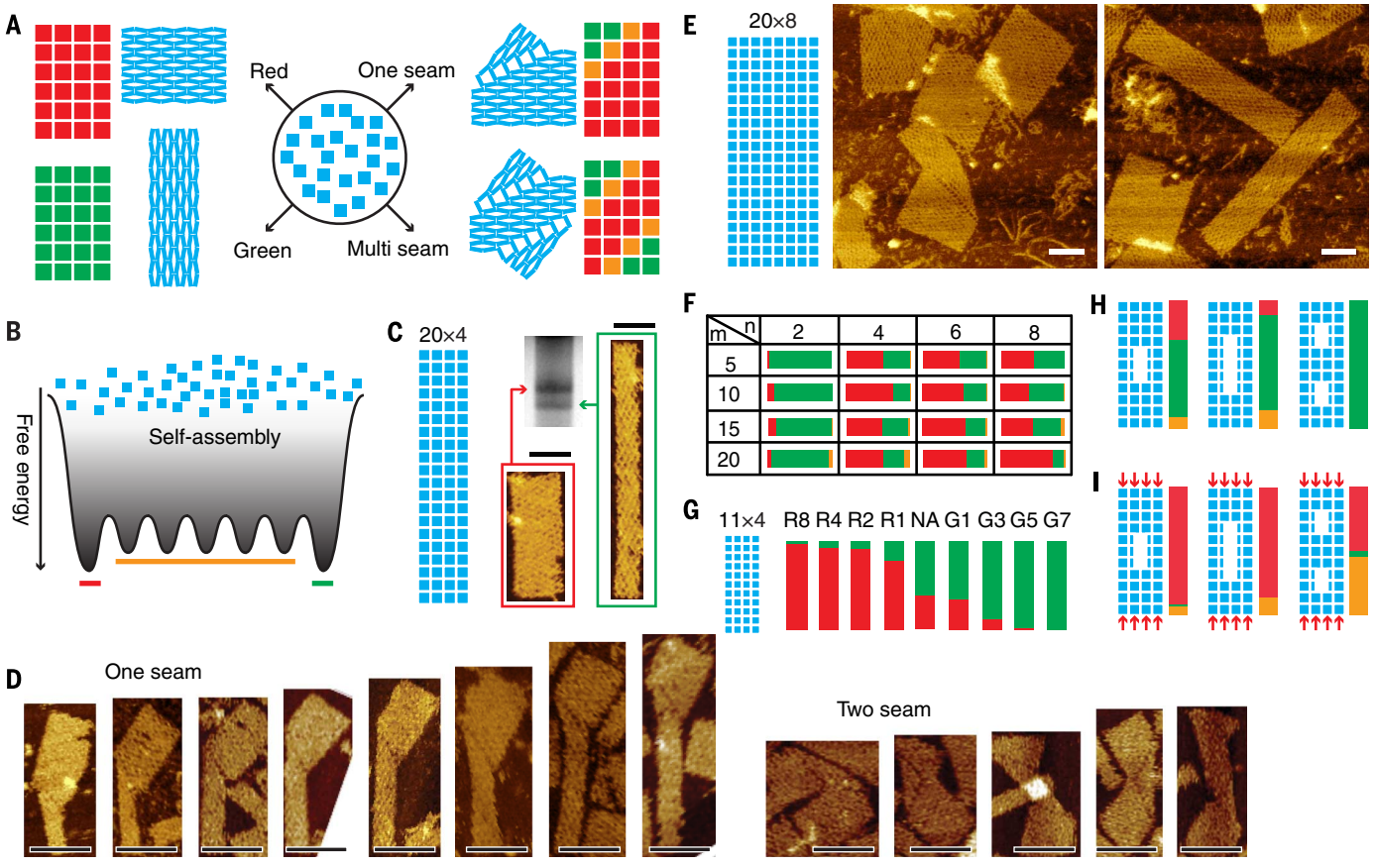

Fig. 2. One-pot assembly of 42-bp DNA-brick relay arrays. (**A**) Multiple conformations result from assembly of a DNA-brick relay array: "red array" conformation, "green array" conformation, and "mixed array" conformations, which contains units with red conformation, green conformation, and orange conformation. The orange units (corresponding to a higher-energy, unstable state) form diagonal seams that bridge together the red units and the green units. (**B**) Proposed, simplified energy landscape of assembly. The units assemble into the two global energy minima corresponding to the red array conformation and the green array conformation, and local energy minima corresponding to the mixed array conformations. (**C**) Assembly of the 20 × 4 42-bp DNA-brick relay array results in two (red array and green array) dominant products in the agarose gel. (**D**) AFM images of mixed array conformations of the 20 × 4 42-bp DNA-brick relay array. (**E**) The 20 × 8 42-bp DNA-brick relay array is used as a "canvas" to generate relay arrays of different sizes and aspect ratios. (**F**) Percentages of red array conformation, green array conformation, and mixed array conformation of $m \times n$ relay arrays. (**G**) Numbers (n) of red triggers (Rn) and green triggers (Gn) shift the assembly result of the 11 × 4 42-bp DNA-brick relay array. (**H**) Removal of units from the 11 × 4 42-bp DNA-brick relay array alters the assembly result. (**I**) A combination of unit removal and addition of eight red triggers affects the assembly result. Scale bars, 50 nm.

each four-way junction. The assembly results showed a strong correlation between the junction sequences (and thus the base stacking) and the red/green (R/G) ratios. In good agreement with our estimate, the green array was the dominant conformation (R/G = 0.24) for design I, while the red array was the dominant conformation (R/G = 3.0) for design II.

Transformation of DNA-origami relay array

To identify a suitable design for our study of DNA array transformation, we compared different DNA-brick relay arrays and DNA-origami relay arrays. Overnight room-temperature incubation of red trigger strands with a preassembled 11 × 4 42-bp DNA-brick relay array, an 8 × 5 52-bp DNA-brick relay array, and a 10 × 4 64-bp DNA-brick relay array (fig. S21) did not convert a noticeable

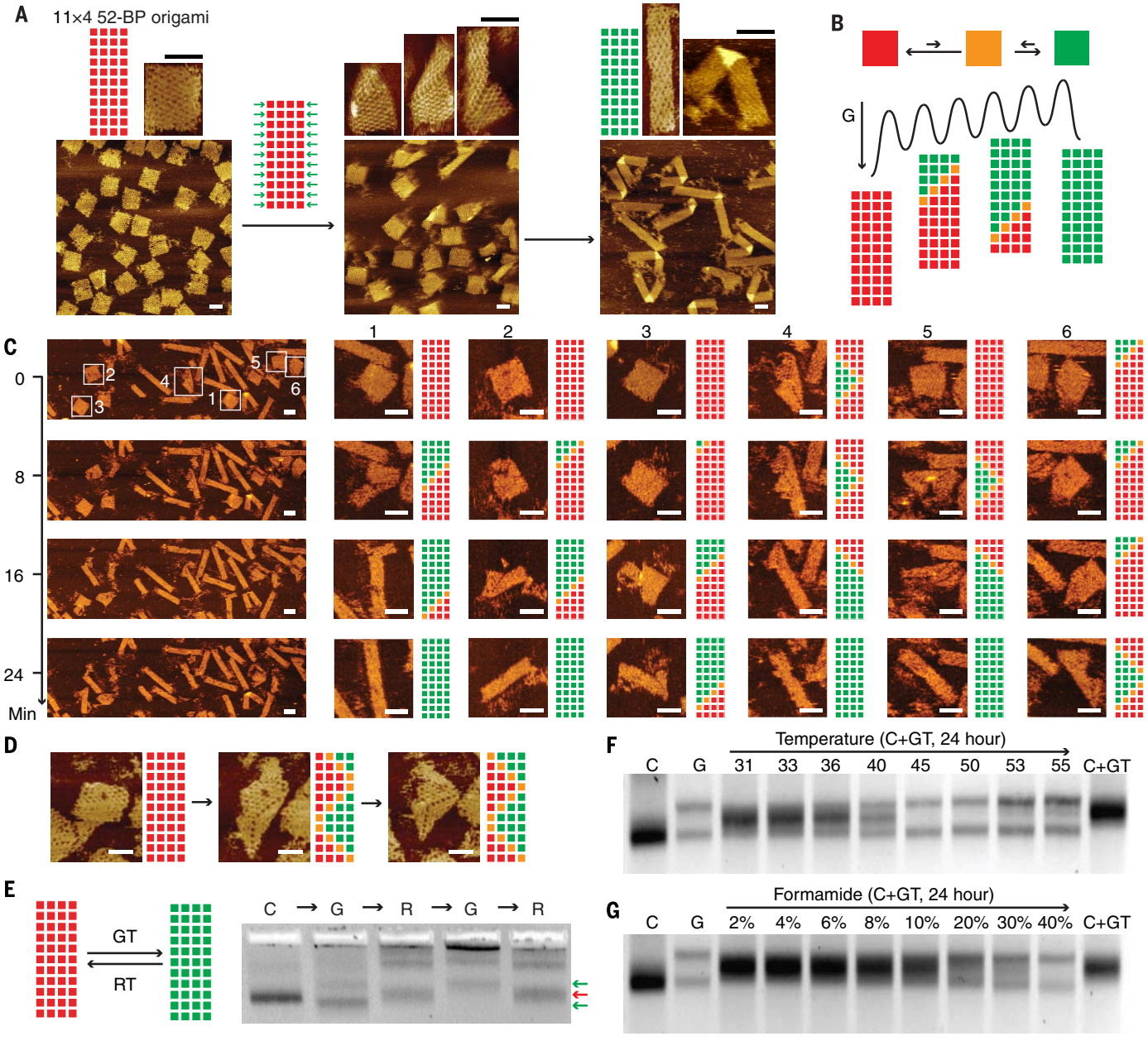

Fig. 3. Transformation of DNA-origami relay arrays. (**A**) An 11 × 4 52-bp DNA-origami relay array forms predominantly red array conformations. Subsequent addition of 22 green triggers converted the red array conformation to the mixed array conformation, then to the green array conformation. Some of the green arrays are folded because of the tension generated by the free scaffold. (**B**) The 52-bp DNA-origami relay array showed a greater tendency to form red array conformations than green array conformations. (**C**) AFM images (4-min scan time per frame) show real-time transformation of the relay array from red array conformations to green array conformations in the presence of 22 green triggers. The transformation was mostly initiated at a corner, although sometimes from the middle section of an edge, and followed the diagonal pathways. (**D**) Occasionally the transformation was initiated at separate, multiple locations. (**E**) The red/green array transformation is a reversible process, which can be repeated multiple times by removal of previous triggers and addition of new triggers. Arrows indicate the product bands. Note that the green array conformation has two bands. (**F** and **G**) The kinetics are accelerated by elevated temperature (F) or formamide concentration (G) for the transformation from the red array conformation to the green array conformation. Lane C: Relay array assembled without trigger. Lane G: Relay array assembled with 22 green triggers. The slower-mobility band corresponds to the folded green array conformation in (A). Lane C+GT: 22 green triggers (GT) were added to a preassembled relay array (C), and immediately loaded into the gel. It appears that the triggers quickly bind to the array, causing a shift of mobility. Scale bars, 50 nm.

percentage of green array conformation to red array conformation. The arrays were then incubated at higher temperatures or in solutions containing higher concentrations of formamide to accelerate the transformation kinetics, but the DNA-brick relay array started to show damage at 55°C or 40% formamide before noticeable transformation was observed.

We then turned our attention to DNA-origami relay arrays, which may be more resilient to denaturing conditions because of the long scaffold strand. We assembled an 11 × 7 32-bp DNA-origami relay array (fig. S22) and an 11 × 4 52-bp DNA-origami relay array with a p7560 scaffold. Both arrays resulted in only the red array conformation. It is unknown how the scaffold (about half the molecular weight of the whole array) might affect the formation and transformation of the DNA-origami relay array, and the scaffold dependence of the DNA-origami relay array requires further study. We eventually chose the 52-bp DNA-origami relay array for real-time transformation, as subsequent studies revealed that this relay array is easiest to transform and is convenient for image analysis.

Transformation of preassembled 11×4 52-bp DNA-origami relay array in the red conformation was initiated by the addition of 22 green trigger strands. The arrays initially transformed to mixed conformations at 45°C, then to ~100% green array conformations at 55°C (Fig. 3A). Analysis of the mixed array conformations revealed that the dominant pathway of transformation is diagonal, consistent with the results for DNA-brick relay arrays. Based on the results of the transformation from the red array conformation to the green array conformation, we made the assumption that the red unit conformation was slightly favored over the green unit conformation in the p7560 DNA-origami relay array, resulting in a tilted energy landscape for the transformation process (Fig. 3B and fig. S23).

Real-time AFM was used to study the in situ single-molecule transformation of the DNA relay arrays (Fig. 3C and fig. S24). Within a 30-min scan, multiple array transformations were observed. The transformation appeared to be a stochastic process: Most of the transformations started from a corner and propagated through a diagonal pathway, while a smaller number of transformations were initiated from the edges and propagated along a "swallowtail" pathway. In rare cases, transformation of an array was also observed being initiated at multiple locations (Fig. 3D).

The transformation of the 52-bp DNA-origami relay array is reversible. Using modified trigger strands with toehold extensions and corresponding release strands, we demonstrated multiple conversions between the red array conformation and the green array conformation (Fig. 3E and fig. S25). The green array conformation has two product bands: The upper band and the lower band correspond to the folded structure [due to the tension generated by the free scaffold (*46*)] and open structure, respectively, in Fig. 3A. We observed that the "open" green conformation is more dominant than the "folded" green conformation after the initial assembly. However, after the array's transformation to red, and then back to green, nearly 100% of arrays turned into the folded green conformation. The underlying reason for this conversion needs further investigation.

The kinetics of the transformation can be accelerated by either increasing temperatures (Fig. 3F) or using higher concentrations of formamide (Fig. 3G), likely because of the reduced energy needed to break the base-stacking interactions under these denaturing conditions [e.g., increasing the temperature reduces the base-stacking energy from an average of –5.2 kJ/mol at 32°C to –2.9 kJ/mol at 52°C (*47*)]. The real-time transformation in Fig. 3C was acquired by using DNA-origami relay arrays in a 10% formamide solution. We also observed real-time transformation of an 11 × 4 32-bp DNA origami array at 65°C using a temperature-controlled AFM (*48*) (fig. S26). However, the AFM images are much noisier at such a high temperature. The kinetics of transformation can also be increased by the mechanical disturbance induced by the AFM tip, as shown in fig. S27. The transformations occurred at higher frequencies when the sample was subjected to the contact force from the AFM tip. This AFM tip–enhanced transformation was confined to only the scanned area. This phenomenon may provide a means to manipulate our dynamic DNA arrays at specific locations.

Regulation of transformation in DNA relay arrays

With a better understanding of the factors affecting transformation, we extended our study to control the transformation of the DNA-origami relay arrays. We demonstrated that transformation could be initiated at selected locations, blocked, and controlled using arrays with different shapes.

The transformation can be initiated at prescribed locations on the 11 × 4 52-bp DNA origami relay array. Using real-time AFM, we demonstrated initiation of transformation from a corner or from the middle of an edge with five green trigger strands and subsequent propagation of the new conformation (Fig. 4A and fig. S28). Both the number and locations of trigger strands affect the initiation of array transformation and the degree of transformation. A detailed study is included in fig. S29. With three or fewer trigger strands added in a corner, the transformation process could not be initiated. Increasing the number of trigger strands to six or eight triggered partial conversion to mixed array conformations, with a small number of green array conformations. The addition of 11 green trigger strands led to full transformation to the green conformation for most of the arrays. Adding trigger strands to the corners appeared to be more effective at inducing transformation than adding the same number of triggers to the edges (fig. S29B). In addition, adding both red trigger and green trigger strands can lead to transformation to specific mixed array conformations (fig. S29C). We also compared the transformation efficiency of preassembled arrays using a one-pot assembly in the presence of triggers. As expected, the results showed that conversion was typically more complete under the one-pot assembly condition (fig. S30).

We also explored two strategies to turn off or turn on transformation at selected locations by blocking or resuming the information pathways between units. In the first approach, we created an "off" function by removing one unit from the relay array, which creates a local energy minimum (Fig. 4B and fig. S31) that traps the array transformation. Reintroduction of the missing unit enables the transformation to escape the trap and proceed (Fig. 4B). We further demonstrated the blocking and resuming of transformation at different locations on the array using this strategy (Fig. 4C and fig. S32). In the second approach, we showed that this "off" function can also be achieved by using a "lock" strand (Fig. 4D). This strand binds to single-stranded DNA extensions from two neighboring units, effectively locking the units into a fixed conformation (fig. S33).

Information relay in an DNA relay array can also be programmed by removal or addition of antijunction units. Using the 11 × 4 52-bp DNA-origami relay array as a canvas, we demonstrated a "2" shaped array by removing eight units. (Fig. 4E and fig. S34). After the initiation of transformation at the top corner, this array transformed in a three-step process: The addition of two initial corner triggers transferred the array only up to the top-right corner; five additional triggers were added to the top-right corner to push the transformation about halfway through the array; finally, the array transformation was completed after the subsequent addition of another five triggers. Each step was verified in AFM images.

Spontaneous transformation of both DNA-brick relay array and DNA-origami relay array without addition of triggers was occasionally observed during the AFM scan in the presence of 10 to 30% formamide (fig. S35), but an in-depth study of this rare and random phenomenon was not pursued in this work.

We then studied how the transformation of DNA-origami relay arrays is influenced by connecting the arrays into monomer tubes, and into oligomer 1D chains and tubes. We substituted the red triggers for connector strands that link the top and bottom edges of the 11 × 4 52-bp DNA-origami relay array (fig. S36). The relay array assembly with the connectors resulted in a red-conformation nanotube, which could convert to a green-conformation tube after addition of 22 green trigger strands (Fig. 4F). In comparison to the 2D relay arrays, unit conversion in the nanotube was more cooperative. A two-step process was observed: first, the tube was converted to a stable state in which most units appeared partially open at 40°C (Fig. 4F and 4G, top); then, the tube was fully converted to a green-conformation tube at 50°C (Fig. 4F and 4G, bottom). Further discussion, AFM images, and transmission electron microscopy (TEM) images are shown in fig. S37A. By contrast, one-pot assembly of the array with both the connectors and green triggers did not produce green-conformation tubes (figs. S37B and S38).

Instead, oligomer tubes and 1D chains of arrays were observed (Fig. 4H and fig. S39). This behavior differs from that of a previous work in which an origami tube design formed two isomers in one-pot assembly (*49*). This is likely because the addition of more green triggers should favor interarray connections over intra-array connections, owing to the increased rigidity (it is harder to bend the green array conformation). With six green triggers, the assembly resulted in red-conformation oligomer tubes and 1D chains. When 10 green triggers were added to the middle of the array, the assembly produced mostly oligomer 1D chains with mixed red and green conformations. When 11 green triggers were added to one side of the array, assembly resulted in green-conformation 1D chains.

Discussion

Our work has demonstrated a general strategy for the construction of large DNA relay arrays with interconnected modular structural components. Each component is a dynamic unit that can transfer its structural information to neighboring components. Through the study of these DNA relay arrays, we have demonstrated controlled, multistep, long-range transformation of the DNA arrays. This dynamic behavior can be regulated by the shapes and sizes of arrays, by external factors (e.g., temperature), by the initiation of transformation at selected units, and by the information propagation pathways.

A next step would be to extend the DNA relay arrays to 3D spaces, larger sizes, more intricately shaped designs, and more complex dynamic

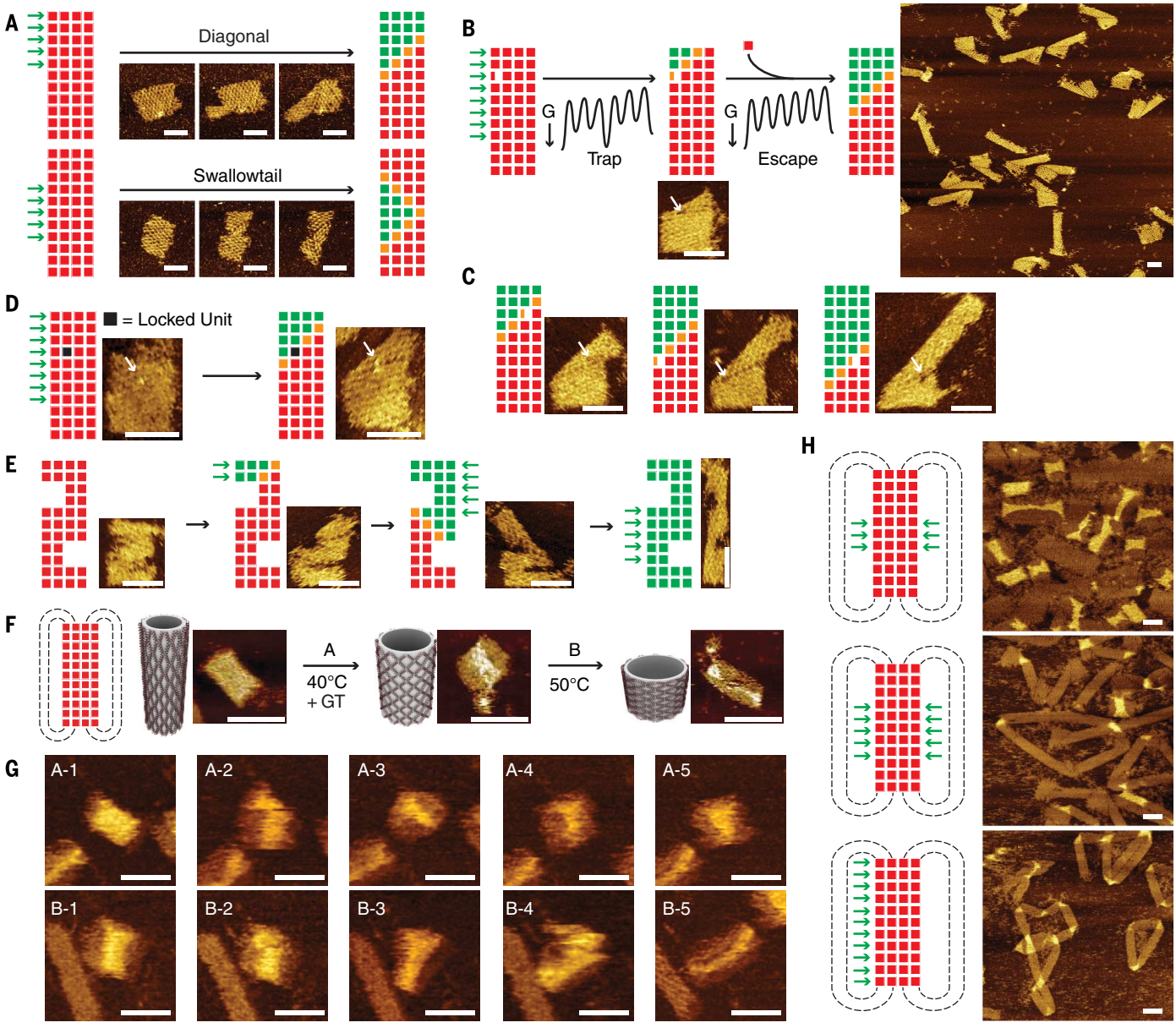

Fig. 4. Controlled transformation of DNA-origami relay arrays. (**A**) Control of the initiation of transformation via selection addition of green triggers (**B**) The transformation pathways can be blocked and resumed by the removal and addition of units. (**C**) The transformation can be blocked at any designated location. (**D**) Blocking of transformation pathways via "lock" strands. (**E**) Control of the transformation pathway using shape design. (**F**) Transformation of a closed design is more cooperative. A stable conformation in which all units are partially open was observed at 40°C. (**G**) Real-time AFM images of transformation from the red array conformation tube to the mixed array conformation tube (A-1 to A-5), and from the mixed array conformation tube to the green array conformation tube (B-1 to B-5). (**H**) Addition of green triggers in one-pot assembly reduced, and eventually eliminated, the red array tube formation. Scale bars, 50 nm.

behaviors. In fig. S40, we show a small 3D DNA-brick relay array design, which consists of two sets of dynamic junctions, perpendicular to each other. As expected, this 3D DNA-brick relay array produced three detectable conformations, confirmed by TEM images. In a previous work, we successfully produced canonical nonreconfigurable 3D DNA-brick structures up to ~12,000 bp (*27*). Assuming that reconfigurable structures with a similar size could be made, the largest structure would contain ~142 42-bp antijunction units. Such large, intricate structures would enable demonstration of complicated transformation in 3D space. Hierarchical assembly of multiple DNA relay arrays may lead to construction of larger and more intricate designs. In addition, more complex information pathways (e.g., multibranched pathways) in DNA relay arrays and sequence-dependent behavior of DNA relay arrays will require further study.

We expect that our new DNA dynamic arrays will shed light on how to construct nanostructures with increasing size and complex dynamic behaviors, and may enable a range of applications using dynamic DNA arrays. For example, the transformation propagation in the DNA relay arrays resembles crucial features of allosteric mechanisms that are observed in biological systems (*50*). Therefore, our artificial arrays may serve as model structures to investigate and validate underlying mechanisms of allostery (*51*, *52*), or be used to design and construct allosteric metamaterials (*53*). The DNA relay arrays may also be used as a platform to analyze biomolecular interactions at a single-molecule level (*46*, *54*–*56*), by translating and amplifying the molecular interactions to conformational changes in the DNA relay arrays or to subsequent molecular events (e.g., chemical reactions, fluorescence resonance energy transfer, etc.). A potential limitation of current DNA relay arrays for biological applications is the slow kinetics of array transformations under mild conditions that are compatible with biomolecules. This challenge may be overcome by the development of next-generation DNA relay arrays through engineering of the structural units and array sequences. In addition, rational sequence design may be used in DNA-brick relay arrays to study the binding energy of the junctions (*57*, *58*), which could enable more sophisticated control of the assembly and transformation of the DNA relay arrays. DNA nanostructures have long been used to construct functional structures and devices by scaffolding the arrangement of proteins, nanoparticles, and other functional materials with nanoscale precision (*59*). The ability to construct large DNA structures with controlled, complex, long-range information relay and dynamic behavior should improve the sophistication and functionality of such hybrid functional structures.

Materials and methods

DNA synthesis

The single-stranded M13 bacteriophage (p7560) scaffold was produced following a published protocol (*23*). Chemically synthesized DNA oligomers were purchased from Integrated DNA Technologies (www.idtdna.com) and were used without further purification. All other reagents were purchased from Sigma-Aldrich (St. Louis, MO).

DNA relay array design

The DNA-origami relay arrays were designed by using caDNAno (*60*). The DNA-brick arrays were designed by using a modified version of software described previously (*27*).

Sample preparation

For 42-bp DNA-brick relay arrays, DNA strands were mixed at equal molar ratio at a final concentration of 100 nM per strand in 1× TE buffer (5 mM Tris, 1 mM EDTA, pH 8.0), supplemented with 5 to 50 mM $MgCl_2$, and then the mixture was subjected to a one-step isothermal-annealing over 18 hours. The optimal isothermal annealing condition was found to be 53°C incubation for 18 hours in 1× TE buffer with 10 mM $MgCl_2$. For 52- and 64-bp DNA-brick relay arrays, DNA strands were mixed at equal molar ratio at a final concentration of 100 nM per strand in 1× TE buffer with 10 mM $MgCl_2$. Then the samples were subjected to a 20-hour thermal annealing protocol: 95°C for 5 min, from 85° to 24°C at a rate of 20 min/°C. For DNA origami relay arrays, the mixture of staple strands (final concentration: 100 nM of each strand) and the scaffold (final concentration: 10 nM) were mixed in 1× TE buffer, supplemented with 12 mM $MgCl_2$. The samples were then annealed for 10 hours using the following thermal annealing protocol: 95°C for 5 min, from 85° to 24°C at a rate of 10 min/°C.

Agarose gel electrophoresis and purification

Samples were subjected to 0.3 to 3% agarose gel electrophoresis at 60 V for 2 to 7 hours in an ice water bath. Gels were prepared with 0.5× TBE buffer containing 10 mM $MgCl_2$ and with 0.005% (v/v) ethidium bromide. For purification, the target gel bands were excised and placed into a Freeze 'N Squeeze column (Bio-Rad Laboratories, Inc.). The gel pieces were crushed into fine pieces with a pestle in the column, and the column was then centrifuged at 7000*g* for 5 min. Samples that were extracted through the column were collected for TEM or AFM imaging.

AFM imaging

For typical AFM imaging, samples were prepared by deposition of a 2 μl DNA array sample onto freshly cleaved mica. The sample area was then filled with ~80 μl of 1× TE buffer with 112 mM $MgCl_2$. Commercial silicon nitride cantilevers with integrated sharpened tips (Bruker, SNL-10) were used. The topographic images were captured by peak force tapping mode experiments on a Multimode VIII system (Bruker Corporation, Santa, Barbara, CA) in liquid.

TEM imaging

To visualize the samples, we deposited 3 μl of purified samples on glow-discharged, carbon-coated TEM grids for 2 min. Samples were then stained for 1 min with 2% uranyl formate solution containing 25 mM NaOH and subsequently imaged using the JEOL JEM-1400 TEM operated at 80 kV.

DNA relay array transformation in solution

For transformation in aqueous solution, excessive trigger strands (~10 to 20 nM) were added to the purified DNA samples (~5 nM). The mixed samples were then incubated at constant temperatures (from room temperature to 60°C) for 5 min to 12 hours. The samples were then subjected to agarose gel electrophoresis assay or deposited on mica for AFM imaging.

Real-time imaging of DNA relay array transformation in solution

For real-time imaging, the purified DNA samples (~5 nM) were first mixed with an excess of trigger strands (generally ~10 to 20 nM) for 1 min and then deposited on mica.

Imaging in formamide: A solution of 80 μl of 1×TE, supplemented with 12 mM $MgCl_2$ and 10 to 30% formamide, was added to the DNA sample on the mica surface. After incubation for ~5 min, the AFM cantilever was brought close to the mica surface at a relatively low force, and started to scan the samples until no further transformation of DNA arrays was observed in the scan area.

Imaging using temperature-controlled AFM: For real-time imaging via thermal control AFM, the images were acquired with a commercial Multimode Microscope V (Digital Instruments, Santa Barbara, CA) in conjunction with a temperature controller. Temperature variation was accomplished via a resistive heating stage (temperature range: ambient temperature to 250°C, resolution: 0.1°C). A cooling water fluid circuit refrigerates the piezo scanner. Then, DNA array samples were scanned at 60°C until no further transformation of DNA arrays was observed in the scan area.

REFERENCES AND NOTES

1. N. C. Seeman, DNA in a material world. *Nature* **421**, 427–431 (2003). doi: 10.1038/nature01406; pmid: 12540916
2. S. H. Park *et al*., Three-helix bundle DNA tiles self-assemble into 2D lattice or 1D templates for silver nanowires. *Nano Lett.* **5**, 693–696 (2005). doi: 10.1021/nl050108i; pmid: 15826110
3. R. Schulman, E. Winfree, Synthesis of crystals with a programmable kinetic barrier to nucleation. *Proc. Natl. Acad. Sci. U.S.A.* **104**, 15236–15241 (2007). doi: 10.1073/pnas.0701467104; pmid: 17881584
4. P. Yin *et al*., Programming DNA tube circumferences. *Science* **321**, 824–826 (2008). doi: 10.1126/science.1157312; pmid: 18687961
5. H. Yan, S. H. Park, G. Finkelstein, J. H. Reif, T. H. LaBean, DNA-templated self-assembly of protein arrays and highly conductive nanowires. *Science* **301**, 1882–1884 (2003). doi: 10.1126/science.1089389; pmid: 14512621
6. D. Liu, S. H. Park, J. H. Reif, T. H. LaBean, DNA nanotubes self-assembled from triple-crossover tiles as templates for conductive nanowires. *Proc. Natl. Acad. Sci. U.S.A.* **101**, 717–722 (2004). doi: 10.1073/pnas.0305860101; pmid: 14709674
7. P. W. K. Rothemund *et al*., Design and characterization of programmable DNA nanotubes. *J. Am. Chem. Soc.* **126**, 16344–16352 (2004). doi: 10.1021/ja044319l; pmid: 15600335
8. F. Mathieu *et al*., Six-helix bundles designed from DNA. *Nano Lett.* **5**, 661–665 (2005). doi: 10.1021/nl050084f; pmid: 15826105

9. J. Sharma *et al*., Control of self-assembly of DNA tubules through integration of gold nanoparticles. *Science* **323**, 112–116 (2009). doi: 10.1126/science.1165831; pmid: 19119229
10. Y. Ke *et al*., DNA brick crystals with prescribed depths. *Nat. Chem.* **6**, 994–1002 (2014). doi: 10.1038/nchem.2083; pmid: 25343605
11. E. Winfree, F. Liu, L. A. Wenzler, N. C. Seeman, Design and self-assembly of two-dimensional DNA crystals. *Nature* **394**, 539–544 (1998). doi: 10.1038/28998; pmid: 9707114
12. P. W. K. Rothemund, N. Papadakis, E. Winfree, Algorithmic self-assembly of DNA Sierpinski triangles. *PLOS Biol.* **2**, e424 (2004). doi: 10.1371/journal.pbio.0020424; pmid: 15583715
13. Y. He *et al*., Sequence symmetry as a tool for designing DNA nanostructures. *Angew. Chem. Int. Ed.* **117**, 6852–6854 (2005). doi: 10.1002/ange.200502193; pmid: 16187389
14. T. Gerling, K. F. Wagenbauer, A. M. Neuner, H. Dietz, Dynamic DNA devices and assemblies formed by shape-complementary, non-base pairing 3D components. *Science* **347**, 1446–1452 (2015). doi: 10.1126/science.aaa5372; pmid: 25814577
15. P. Wang *et al*., Programming Self-Assembly of DNA Origami Honeycomb Two-Dimensional Lattices and Plasmonic Metamaterials. *J. Am. Chem. Soc.* **138**, 7733–7740 (2016). doi: 10.1021/jacs.6b03966; pmid: 27224641
16. W. Liu, J. Halverson, Y. Tian, A. V. Tkachenko, O. Gang, Self-organized architectures from assorted DNA-framed nanoparticles. *Nat. Chem.* **8**, 867–873 (2016). doi: 10.1038/nchem.2540; pmid: 27554413
17. J. H. Chen, N. C. Seeman, Synthesis from DNA of a molecule with the connectivity of a cube. *Nature* **350**, 631–633 (1991). doi: 10.1038/350631a0; pmid: 2017259
18. W. M. Shih, J. D. Quispe, G. F. Joyce, A 1.7-kilobase single-stranded DNA that folds into a nanoscale octahedron. *Nature* **427**, 618–621 (2004). doi: 10.1038/nature02307; pmid: 14961116
19. R. P. Goodman *et al*., Rapid chiral assembly of rigid DNA building blocks for molecular nanofabrication. *Science* **310**, 1661–1665 (2005). doi: 10.1126/science.1120367; pmid: 16339440
20. P. W. K. Rothemund, Folding DNA to create nanoscale shapes and patterns. *Nature* **440**, 297–302 (2006). doi: 10.1038/nature04586; pmid: 16541064
21. Y. He *et al*., Hierarchical self-assembly of DNA into symmetric supramolecular polyhedra. *Nature* **452**, 198–201 (2008). doi: 10.1038/nature06597; pmid: 18337818
22. E. S. Andersen *et al*., Self-assembly of a nanoscale DNA box with a controllable lid. *Nature* **459**, 73–76 (2009). doi: 10.1038/nature07971; pmid: 19424153
23. S. M. Douglas *et al*., Self-assembly of DNA into nanoscale three-dimensional shapes. *Nature* **459**, 414–418 (2009). doi: 10.1038/nature08016; pmid: 19458720
24. H. Dietz, S. M. Douglas, W. M. Shih, Folding DNA into twisted and curved nanoscale shapes. *Science* **325**, 725–730 (2009). doi: 10.1126/science.1174251; pmid: 19661424
25. D. Han *et al*., DNA origami with complex curvatures in three-dimensional space. *Science* **332**, 342–346 (2011). doi: 10.1126/science.1202998; pmid: 21493857
26. B. Wei, M. Dai, P. Yin, Complex shapes self-assembled from single-stranded DNA tiles. *Nature* **485**, 623–626 (2012). doi: 10.1038/nature11075; pmid: 22660323
27. Y. Ke, L. L. Ong, W. M. Shih, P. Yin, Three-dimensional structures self-assembled from DNA bricks. *Science* **338**, 1177–1183 (2012). doi: 10.1126/science.1227268; pmid: 23197527
28. R. Iinuma *et al*., Polyhedra self-assembled from DNA tripods and characterized with 3D DNA-PAINT. *Science* **344**, 65–69 (2014). doi: 10.1126/science.1250944; pmid: 24625926
29. E. Benson *et al*., DNA rendering of polyhedral meshes at the nanoscale. *Nature* **523**, 441–444 (2015). doi: 10.1038/nature14586; pmid: 26201596
30. R. Veneziano *et al*., Designer nanoscale DNA assemblies programmed from the top down. *Science* **352**, 1534 (2016). doi: 10.1126/science.aaf4388; pmid: 27229143
31. B. Yurke, A. J. Turberfield, A. P. Mills Jr., F. C. Simmel, J. L. Neumann, A DNA-fuelled molecular machine made of DNA. *Nature* **406**, 605–608 (2000). doi: 10.1038/35020524; pmid: 10949296
32. H. Yan, X. Zhang, Z. Shen, N. C. Seeman, A robust DNA mechanical device controlled by hybridization topology. *Nature* **415**, 62–65 (2002). doi: 10.1038/415062a; pmid: 11780115
33. M. Liu *et al*., A DNA tweezer-actuated enzyme nanoreactor. *Nat. Commun.* **4**, 2127 (2013). pmid: 23820332
34. Y. Ke, T. Meyer, W. M. Shih, G. Bellot, Regulation at a distance of biomolecular interactions using a DNA origami nanoactuator. *Nat. Commun.* **7**, 10935 (2016). doi: 10.1038/ncomms10935; pmid: 26988942
35. W. B. Sherman, N. C. Seeman, A Precisely Controlled DNA Biped Walking Device. *Nano Lett.* **4**, 1203–1207 (2004). doi: 10.1021/nl049527q
36. P. Yin, H. Yan, X. G. Daniell, A. J. Turberfield, J. H. Reif, A unidirectional DNA walker that moves autonomously along a track. *Angew. Chem. Int. Ed.* **43**, 4906–4911 (2004). doi: 10.1002/anie.200460522; pmid: 15372637
37. T. Omabegho, R. Sha, N. C. Seeman, A bipedal DNA Brownian motor with coordinated legs. *Science* **324**, 67–71 (2009). doi: 10.1126/science.1170336; pmid: 19342582
38. P. Yin, H. M. T. Choi, C. R. Calvert, N. A. Pierce, Programming biomolecular self-assembly pathways. *Nature* **451**, 318–322 (2008). doi: 10.1038/nature06451; pmid: 18202654
39. K. Lund *et al*., Molecular robots guided by prescriptive landscapes. *Nature* **465**, 206–210 (2010). doi: 10.1038/nature09012; pmid: 20463735
40. S. F. J. Wickham *et al*., Direct observation of stepwise movement of a synthetic molecular transporter. *Nat. Nanotechnol.* **6**, 166–169 (2011). doi: 10.1038/nnano.2010.284; pmid: 21297627
41. L. Feng, S. H. Park, J. H. Reif, H. Yan, A two-state DNA lattice switched by DNA nanoactuator. *Angew. Chem. Int. Ed.* **42**, 4342–4346 (2003). doi: 10.1002/anie.200351818; pmid: 14502706
42. A. E. Marras, L. Zhou, H.-J. Su, C. E. Castro, Programmable motion of DNA origami mechanisms. *Proc. Natl. Acad. Sci. U.S.A.* **112**, 713–718 (2015). doi: 10.1073/pnas.1408869112; pmid: 25561550
43. J. R. Burns, A. Seifert, N. Fertig, S. Howorka, A biomimetic DNA-based channel for the ligand-controlled transport of charged molecular cargo across a biological membrane. *Nat. Nanotechnol.* **11**, 152–156 (2016). doi: 10.1038/nnano.2015.279; pmid: 26751170
44. R. J. Brownlie, R. Zamoyska, T cell receptor signalling networks: Branched, diversified and bounded. *Nat. Rev. Immunol.* **13**, 257–269 (2013). doi: 10.1038/nri3403; pmid: 23524462
45. S. M. Du, S. Zhang, N. C. Seeman, DNA junctions, antijunctions, and mesojunctions. *Biochemistry* **31**, 10955–10963 (1992). doi: 10.1021/bi00160a003; pmid: 1332747
46. P. C. Nickels *et al*., Molecular force spectroscopy with a DNA origami-based nanoscopic force clamp. *Science* **354**, 305–307 (2016). doi: 10.1126/science.aah5974; pmid: 27846560
47. P. Yakovchuk, E. Protozanova, M. D. Frank-Kamenetskii, Base-stacking and base-pairing contributions into thermal stability of the DNA double helix. *Nucleic Acids Res.* **34**, 564–574 (2006). doi: 10.1093/nar/gkj454; pmid: 16449200
48. J. Song *et al*., Direct visualization of transient thermal response of a DNA origami. *J. Am. Chem. Soc.* **134**, 9844–9847 (2012). doi: 10.1021/ja3017939; pmid: 22646845
49. M. Endo *et al*., Helical DNA origami tubular structures with various sizes and arrangements. *Angew. Chem. Int. Ed.* **53**, 7484–7490 (2014). doi: 10.1002/anie.201402973; pmid: 24888699
50. J.-P. Changeux, The feedback control mechanisms of biosynthetic L-threonine deaminase by L-isoleucine. *Cold Spring Harb. Symp. Quant. Biol.* **26**, 313–318 (1961). doi: 10.1101/SQB.1961.026.01.037; pmid: 13878122
51. J.-P. Changeux, S. J. Edelstein, Allosteric mechanisms of signal transduction. *Science* **308**, 1424–1428 (2005). doi: 10.1126/science.1108595; pmid: 15933191
52. O. Schueler-Furman, S. J. Wodak, Computational approaches to investigating allostery. *Curr. Opin. Struct. Biol.* **41**, 159–171 (2016). doi: 10.1016/j.sbi.2016.06.017; pmid: 27607077
53. L. Yan, R. Ravasio, C. Brito, M. Wyart, Architecture and coevolution of allosteric materials. *Proc. Natl. Acad. Sci. U.S.A.* **114**, 2526–2531 (2017). doi: 10.1073/pnas.1615536114; pmid: 28223497
54. Y. Ke, S. Lindsay, Y. Chang, Y. Liu, H. Yan, Self-assembled water-soluble nucleic acid probe tiles for label-free RNA hybridization assays. *Science* **319**, 180–183 (2008). doi: 10.1126/science.1150082; pmid: 18187649
55. S. Rinker, Y. Ke, Y. Liu, R. Chhabra, H. Yan, Self-assembled DNA nanostructures for distance-dependent multivalent ligand-protein binding. *Nat. Nanotechnol.* **3**, 418–422 (2008). doi: 10.1038/nnano.2008.164; pmid: 18654566
56. F. Kilchherr *et al*., Single-molecule dissection of stacking forces in DNA. *Science* **353**, aaf5508 (2016). doi: 10.1126/science.aaf5508; pmid: 27609897
57. S. M. Miick, R. S. Fee, D. P. Millar, W. J. Chazin, Crossover isomer bias is the primary sequence-dependent property of immobilized Holliday junctions. *Proc. Natl. Acad. Sci. U.S.A.* **94**, 9080–9084 (1997). doi: 10.1073/pnas.94.17.9080; pmid: 9256438
58. S. Hohng *et al*., Fluorescence-force spectroscopy maps two-dimensional reaction landscape of the holliday junction. *Science* **318**, 279–283 (2007). doi: 10.1126/science.1146113; pmid: 17932299
59. F. A. Aldaye, A. L. Palmer, H. F. Sleiman, Assembling materials with DNA as the guide. *Science* **321**, 1795–1799 (2008). doi: 10.1126/science.1154533; pmid: 18818351
60. S. M. Douglas *et al*., Rapid prototyping of 3D DNA-origami shapes with caDNAno. *Nucleic Acids Res.* **37**, 5001–5006 (2009). doi: 10.1093/nar/gkp436; pmid: 19531737

ACKNOWLEDGMENTS

We thank M. Dai, S. Jiang, M. Dong, B. Wei, H. Yan, and P. Yin for technical assistance and discussion. This work was supported by NSF CAREER Award DMR–1654485, the Wallace H. Coulter Department of Biomedical Engineering Startup Fund, a Billi and Bernie Marcus Research Award to Y.K., Office of Naval Research grant N00014-15-1-2707 and NSF grant CMMI–1437301 to C.M., and a National Natural Scientific Foundation of China Grant 21605102 to J.S. All data are reported in the main text and supplementary materials.

SUPPLEMENTARY MATERIALS

www.sciencemag.org/content/357/6349/eaan3377/suppl/DC1
Materials and Methods
Figs. S1 to S40
Tables S1 to S13
Movie S1

29 March 2017; accepted 6 June 2017
Published online 22 June 2017
10.1126/science.aan3377

Science

Reconfiguration of DNA molecular arrays driven by information relay

Jie Song, Zhe Li, Pengfei Wang, Travis Meyer, Chengde Mao and Yonggang Ke

Science **357** (6349), eaan3377.
DOI: 10.1126/science.aan3377originally published online June 22, 2017

Relaying information on DNA tiles

Arrays of modular DNA units can relay information by transforming their internal shape in response to binding of DNA trigger strands. Song *et al.* synthesized rectangular arrays of double-stranded DNA (see the Perspective by Yang and Lin). Transient square configurations transform into two stable rectangular structures by pinching across a pair of opposing vertices. Binding of DNA trigger strands causes switching into the alternative stable configuration. The tiles thus create a cascade of transformations along a particular pathway, thereby transmitting information about where binding occurred.

Science, this issue p. eaan3377; see also p. 352